Max-Planck-Institut
für Meteorologie

REPORT No. 40

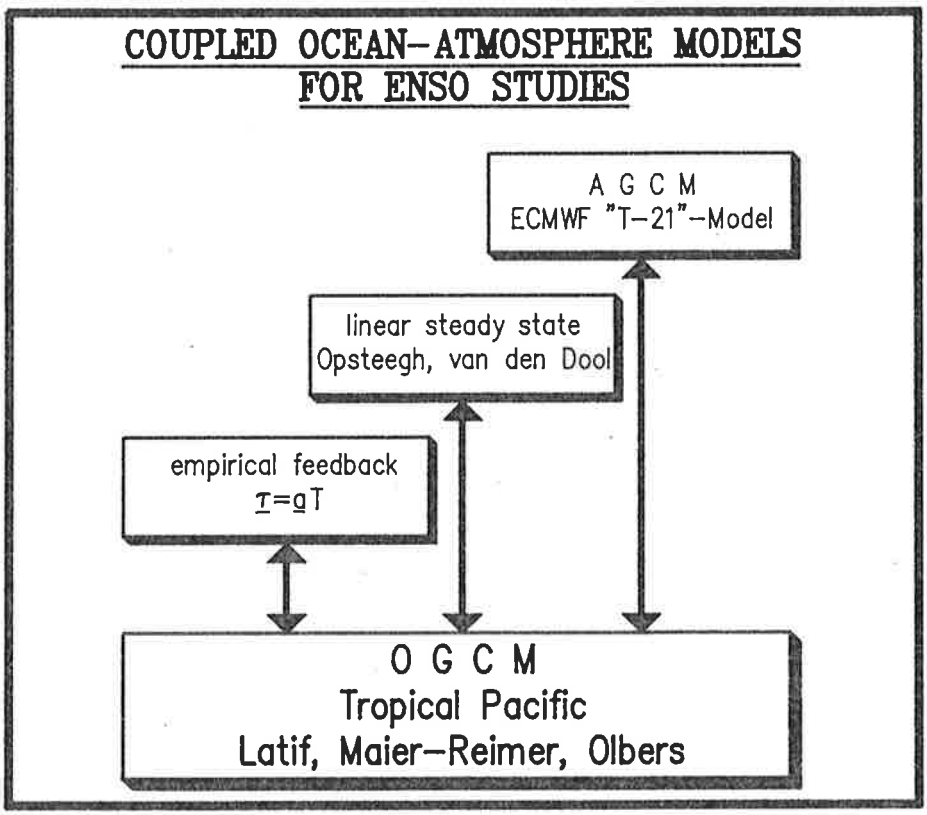

INTERANNUAL VARIABILITY IN THE TROPICAL PACIFIC AS SIMULATED IN COUPLED OCEAN–ATMOSPHERE MODELS

by

MOJIB LATIF • ANDREAS VILLWOCK

HAMBURG, OCTOBER 1989

AUTHORS:

MOJIB LATIF — MAX-PLANCK-INSTITUT FUER METEOROLOGIE

ANDREAS VILLWOCK — MAX-PLANCK-INSTITUT FUER METEOROLOGIE

MAX-PLANCK-INSTITUT
FUER METEOROLOGIE
BUNDESSTRASSE 55
D-2000 HAMBURG 13
F.R. GERMANY

Tel.: (040) 4 11 73-0
Telex: 211092
Telemail: MPI.Meteorology
Telefax: (040) 4 11 73-298

Interannual Variability in the Tropical Pacific as Simulated in Coupled Ocean-Atmosphere Models

M. Latif and A. Villwock

Max-Planck-Institut für Meteorologie
Bundesstr. 55, D 2000 Hamburg 13, F. R. G.

Abstract

The space - time structure of interannual sea level variability simulated with two simplified coupled ocean - atmosphere models is investigated by means of Principal Oscillation Pattern (POP) analysis. Both coupled models consists of an Oceanic General Circulation Model (OGCM) of the tropical Pacific and linear atmospheric feedback. The first coupled model uses an empirical atmospheric feedback derived from data. It simulates low frequency oscillations with periods comparable to the ENSO period of a few years when driven with white noise.

In the second coupled model we use a linear steady state atmosphere model. This coupled model shows quasiperodic oscillations with periods of about 16 months within a certain parameter range.

It is shown that the coupling of ocean and atmosphere is an important contribution for the generation of interannual variability. In both coupled models the interannual variability appears to be linked to the propagation of equatorial waves.

The results are compared to a run with the uncoupled OGCM driven with observed winds. The resulting variability patterns are similar to those in the coupled experiments. The implications of the results for ENSO prediction are discussed.

ISSN 0937-1060

1. Introduction

Interannual variability in the tropical Pacific known as the El Niño/Southern Oscillation (ENSO) phenomenon is gouverned by large scale interactions of ocean and atmosphere. A large number of coupled ocean-atmosphere models have been developed to study these interactions, ranging from simple models (e. g. Hirst (1985), Zebiak and Cane (1987), Battisti and Hirst (1989)) to sophisticated coupled GCMs (e. g. Philander et al. (1988), Gordon (1988), Latif et al. (1988)). 'Intermediate' models have been described by Schopf and Suarez (1988) and Neelin (1988). Each of these coupled models has succeeded in describing certain aspects of ENSO, but none of them has yet been able to simulate ENSO in all its observed complexity.

Several interesting results have been obtained from coupled model integrations, such as the concept of the 'delayed action oscillator', first decribed explicitly by Schopf and Suarez (1988). According to this concept the oscillatory behaviour and the quasiperiodicity of ENSO are due to the propagation of equatorial waves and their reflection at meridional boundaries. This implies that the memory of the coupled ocean-atmosphere system lies entirely in the ocean. Evidence for the 'delayed action oscillator' was found not only in simple models but also in a simulation with a coupled GCM performed by Philander et al. (1988). The authors, however, attributed this result to shortcomings in their atmosphere model.

Other authors (e. g. Lau (1985), Wyrtki (1985)) explain ENSO as an inherent instability in the coupled ocean-atmosphere system triggered by stochastic forcing and strongly modulated by the seasonal cycle. Support for this hypothesis comes from the coupled model simulations of Latif et al. (1988) and Barnett et al. (1989). Latif et al. (1988) showed that strong wind events over the western Pacific can cause persistent large scale anomalous SST in the equatorial Pacific, although this particular coupled model did not simulate self-exited low frequency oscillations. Barnett et al. (1989) showed that anomalous land processes over Eurasia can also cause anomalous SST in the equatorial Pacific, using basically the same coupled model as Latif et al. (1988).

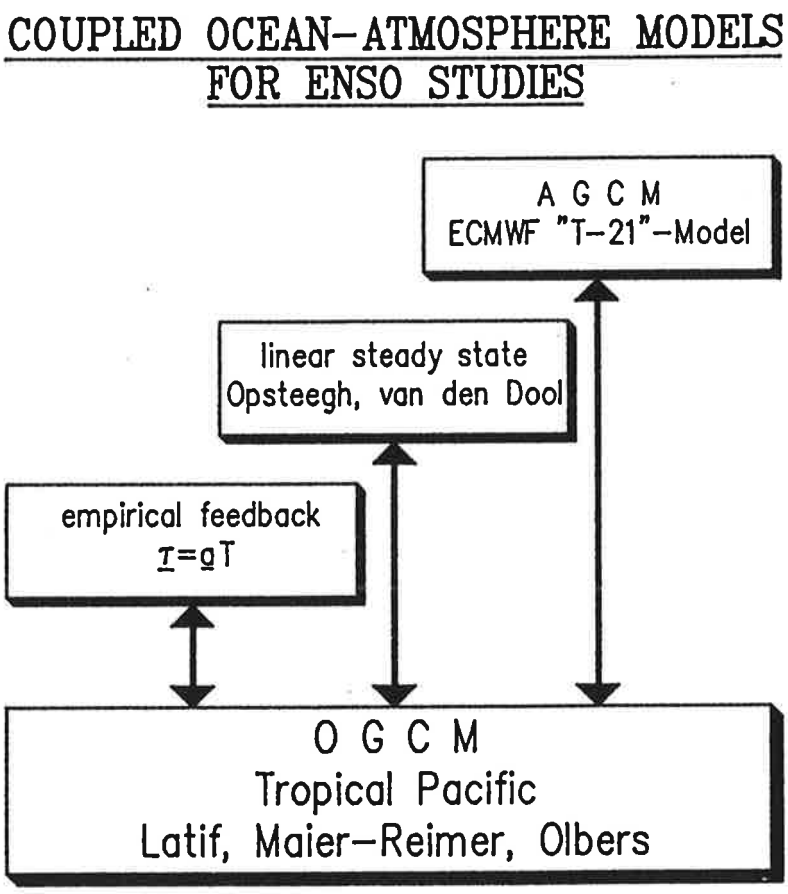

Figure 1: Model hierarchy

In order to investigate the various ENSO mechanisms in more detail we have developed a hierarchy of coupled ocean-atmosphere models (Fig. 1). In this paper we present the two simplified coupled models including only linear atmospheric feedback. The goal of the experiments was to determine their full variability spectrum in extended range integrations. In section 2 we briefly describe the technique of Principal Oscillation Patterns (POPs) used to analyze the variability. In section 3 the ocean model is presented, together with the simulated interannual variability in the tropical Pacific with observed wind stress forcing. In section 4 we describe the two coupled models and the results of the extended range integrations in terms of sea level. Section 5, finally, concludes the paper with a brief summary and a discussion of the results.

2. Principal Oscillation Patterns

To characterize the space-time variability of our simulations we shall use the analysis technique of Principal Oscillation Patterns (POPs) described by Hasselmann (1988), Storch et al. (1988) and Xu and Storch (1989). The POP - technique extracts the principal modes of variability from a multidimensional time series. The POPs are the eigenvectors of the system matrix obtained by fitting the data to a first order Markow process in which the residual forcing is minimized. In general POPs are complex with real and imaginary parts $\mathbf{p}_1$ and $\mathbf{p}_2$. They can describe travelling modes (when the patterns $\mathbf{p}_1$, $\mathbf{p}_2$ are approximately sine and cosine waves in quadrature) or standing waves (when one the patterns is very small). In the genaral case, the POP oscillation is described as the superposition of two patterns representing two standing, damped oscillations in quadrature with each other. The complex eigenvalues define a rotation period P and an e-folding time δ for exponential decay. The time evolution of the POPs ($z_1(t)$, $z_2(t)$) is obtained from the projection of the original time series on the adjoint POPs.

In the original data space the trajectory $\varphi(\underline{x},t)$ of the system is given by:

$$\varphi(\underline{x},t) = z_1(t)\cdot p_1(\underline{x}) + z_2(t)\cdot p_2(\underline{x}) \qquad (1)$$

which leads to the following interpretation: If at a certain time t_0 the system is in the state p_1, it will be at time $t_0+P/4$ in the state $-p_2$, at time $t_0+P/2$ in the state $-p_1$, at time $t_0+3P/4$ in the state p_2, and eventually (if δ is large enough) at time t_0+P back in the state p_1. That is, the system is generating the cyclic sequence of patterns

$$\cdots\cdots\ p_1 \Rightarrow -p_2 \Rightarrow -p_1 \Rightarrow p_2 \Rightarrow p_1\ \cdots\cdots \qquad (2)$$

3. Ocean model

3.1 Model description

The Oceanic General Circulation Model (OGCM) described by Latif et al. (1985) and Latif (1987) is a primitive equation model on an equatorial β-plane representing the tropical Pacific Ocean from 30°N to 30°S. It includes real coastlines but no bottom topography, so that the ocean floor is at a constant depth of 4000 m. The longitudinal resolution is constant with 670 km. In the meridional direction the resolution is variable, increasing from 50 km near the equator to about 400 km at the boundaries. Vertically, there are 13 levels, ten of which are placed within the upper 300 m.

Vertical mixing coefficients are Richardson number dependent (Pacanowski and Philander (1982)). The vertical eddy viscosity and eddy diffusivity were both assigned values of 20 cm^2/s under neutral conditions and have background values of 0.1 and 0.01 cm^2/s, respectively. The horizontal eddy viscosity is constant with a value of 10^8 cm^2/s. Explicit horizontal heat diffusion is not included.

The ocean model is forced by surface wind stress and surface heat flux. The heat flux into the ocean was determined in all experiments from the prescribed

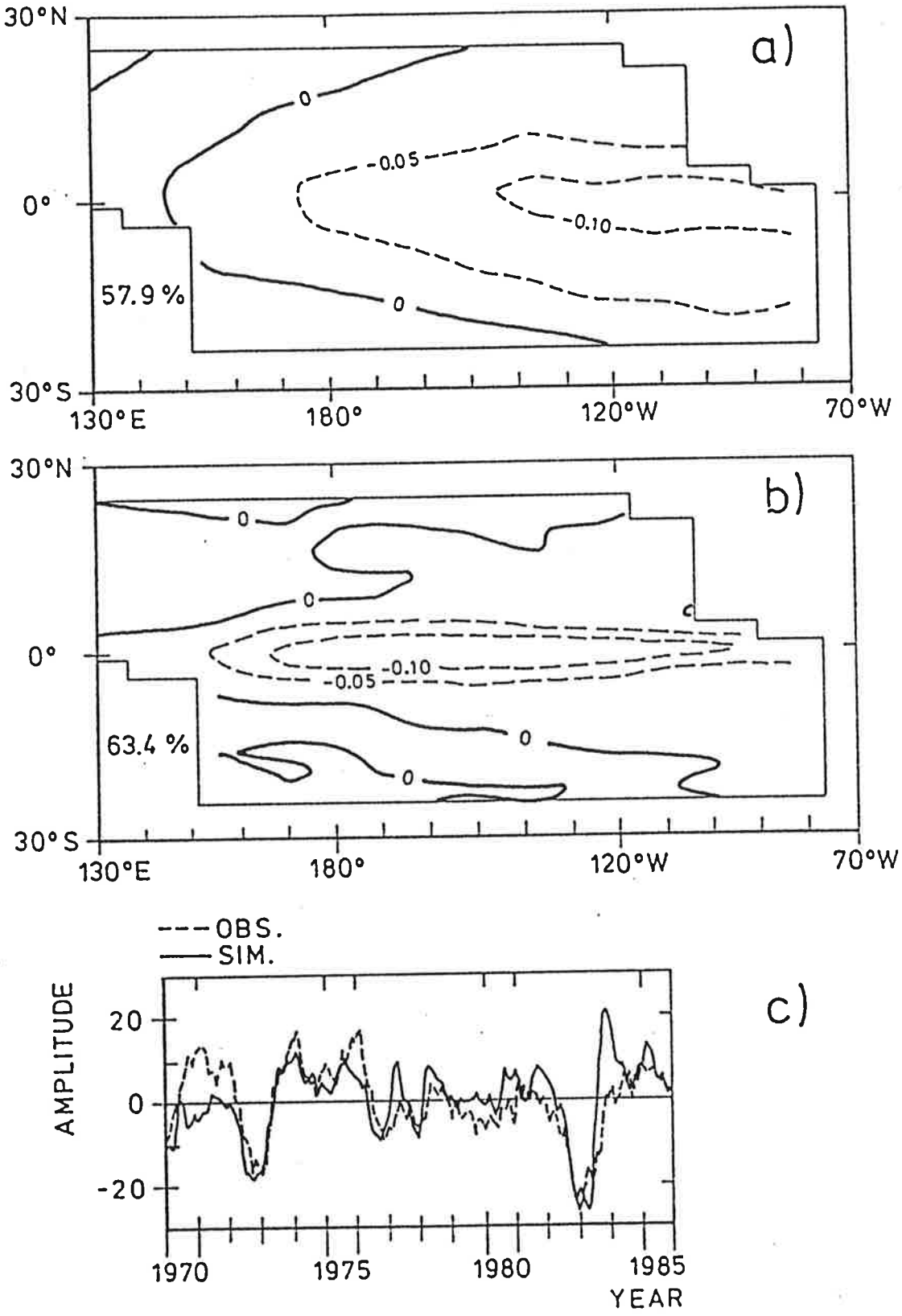

Figure 2: First EOF of observed and simulated SST anomalies. a) Spatial pattern derived from observations, b) spatial pattern derived from the uncoupled model run, c) EOF time series.

climatological near-surface (2 m) air temperature, using a standard Newtonian formulation (Haney (1971)). The feedback parameter was chosen to yield a time constant of about 30 days for the upper layer of 10 m thickness.

3.2 Verification

The ability of the ocean model to simulate interannual variability in the tropical Pacific was investigated by forcing it with observed wind stress for the period 1961 to 1985. The wind data were taken from the Florida State University (FSU) data set (Goldenberg and O'Brien (1981), Legler and O'Brien (1984)). Since the most important oceanic quantity in studies of air-sea interaction is SST, we compare the leading Empirical Orthogonal Functions (EOFs) of simulated and observed SST anomalies (Fig. 2). These are closely related to the ENSO phenomenon, as can be inferred from a comparison of the EOF-coefficient time series (Fig. 2c) with the time series of the Southern Oscillation Index (not shown). Because observed SST anomalies were only available for the period 1970 to 1985, the EOF - analysis of the model data was also restricted to this time period. The first EOF accounts in both observed and simulated data for approximately 60 % of the total variance. The two patterns show large spatial coherence with strongest anomalies at the equator. The anomaly pattern of simulated SSTs (Fig. 2b), however, is more strongly equatorially trapped than the observed pattern (Fig. 2a) and the model simulates maximum anomalies in the central rather than in the eastern Pacific. The two EOF time series (Fig. 2c) are highly coherent with a squared coherence of 0.8 and almost vanishing phase for periods around 40 months (not shown).

In this paper we shall discuss the different simulations in terms of sea level, since this quantity enhances the travelling wave features. It is therefore of special interest to see how this quantity is simulated by the ocean model. It was already shown by Latif (1987) that interannual sea level anomalies at fixed locations are simulated reasonably well. Here we present the leading EOF of simulated sea level anomalies (Fig. 3), which is clearly associated with the ENSO phenomenon (Fig. 3c) and accounts for about 35 % of

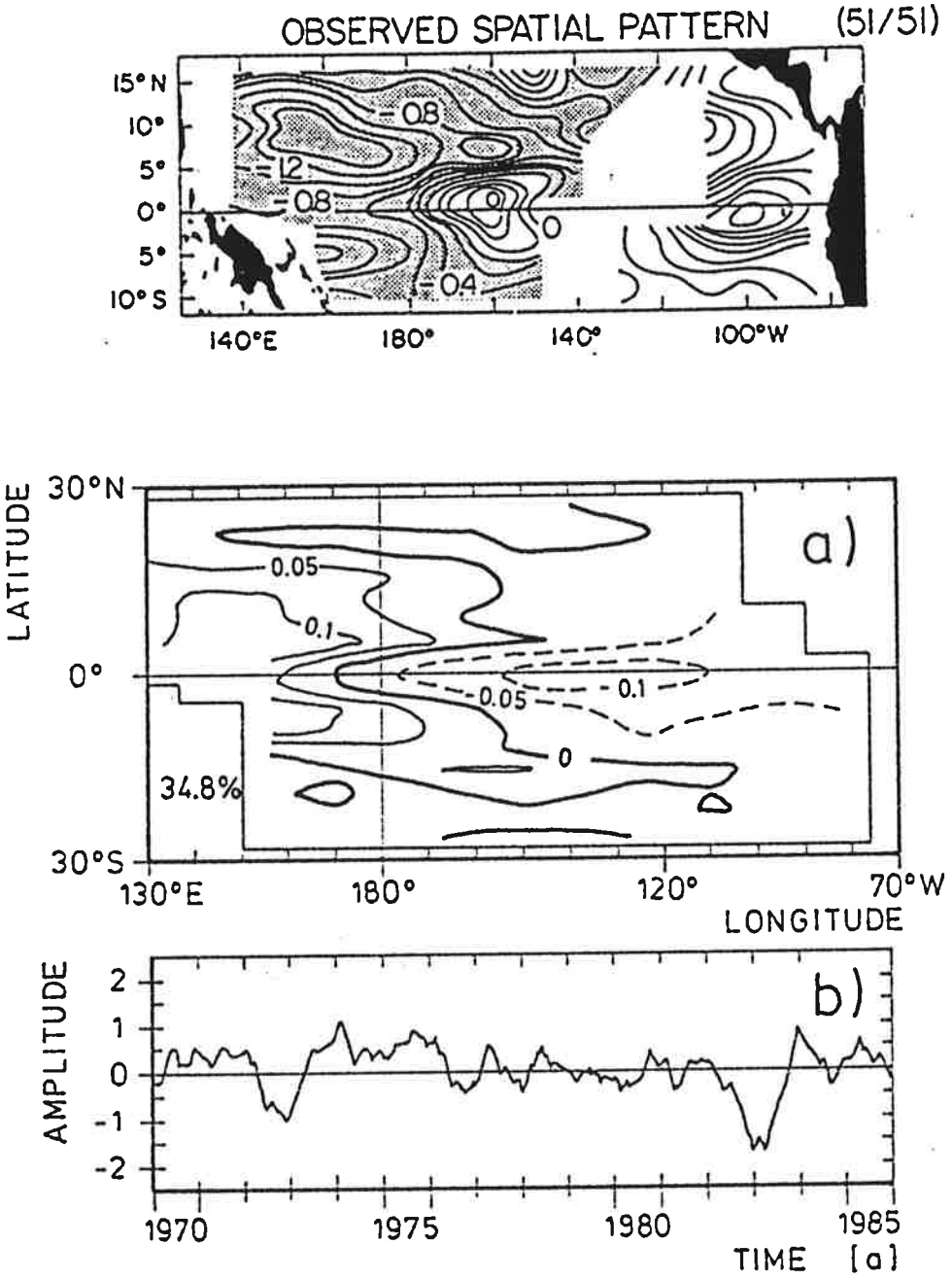

Figure 3: a) Spatial pattern of first EOF of observed anomalous upper layer thickness reproduced from the paper of White and Pazan (1987), b) Spatial pattern of simulated sea level anomalies, c) EOF time series of the pattern presented in b).

the total variance. The simulated spatial pattern (Fig. 3b) shows opposite changes of sea level in the western and eastern Pacific. One finds two off-equatorial maxima in the western Pacific located at about 6° on either side of the equator. Maximum anomalies in the east have similar strength but are centered on the equator. The basic features of our model EOF were also found by Inoue et al. (1987), who carried out an EOF analysis for the observed upper layer thickness (which is closely related to sea level) for the 4-year period 1979 to 1982 (Fig. 3a).

3.3 POP - analysis

The POP - analysis of simulated sea level anomalies was performed for the entire 25-year period 1961 - 1985. Prior to the analysis the data were subjected to band pass filtering retaining variability on time scales between 16 and 60 months.

We found one dominant POP pair (Fig. 4) with rotation period P = 26 months and decay time δ = 69 months describing 33 % of the total variance. This mode is associated with the ENSO phenomenon as can be inferred from the comparison of the coefficient time series (Fig. 4c) with the time series of the 1. EOF of observed SST anomalies (Fig. 2c). The cross spectral analysis of the two POP coefficient time series (not shown) shows that they have same variance and that they are highly coherent for periods of 20 to 50 months (squared coherence > 0.9) with a phase shift of -90°, as expected theoretically.

The imaginary part p_2 of this POP agrees well with the corresponding EOF patterns (Fig. 3a and 3b) and reproduces the observed spatial structure of sea level anomalies during the extremes of ENSO (e. g. during El Niño and La Niña events). The pattern p_2 is characterized by opposite anomalies in the western and eastern equatorial Pacific. Negative anomalies are centered at the equator near 130°W and extend from 170°E to the eastern boundary. Positive anomalies are strongest near 150°E at about 6°N and 6°S, extending in a northeastern and southeastern direction up to the northern and southern boundary.

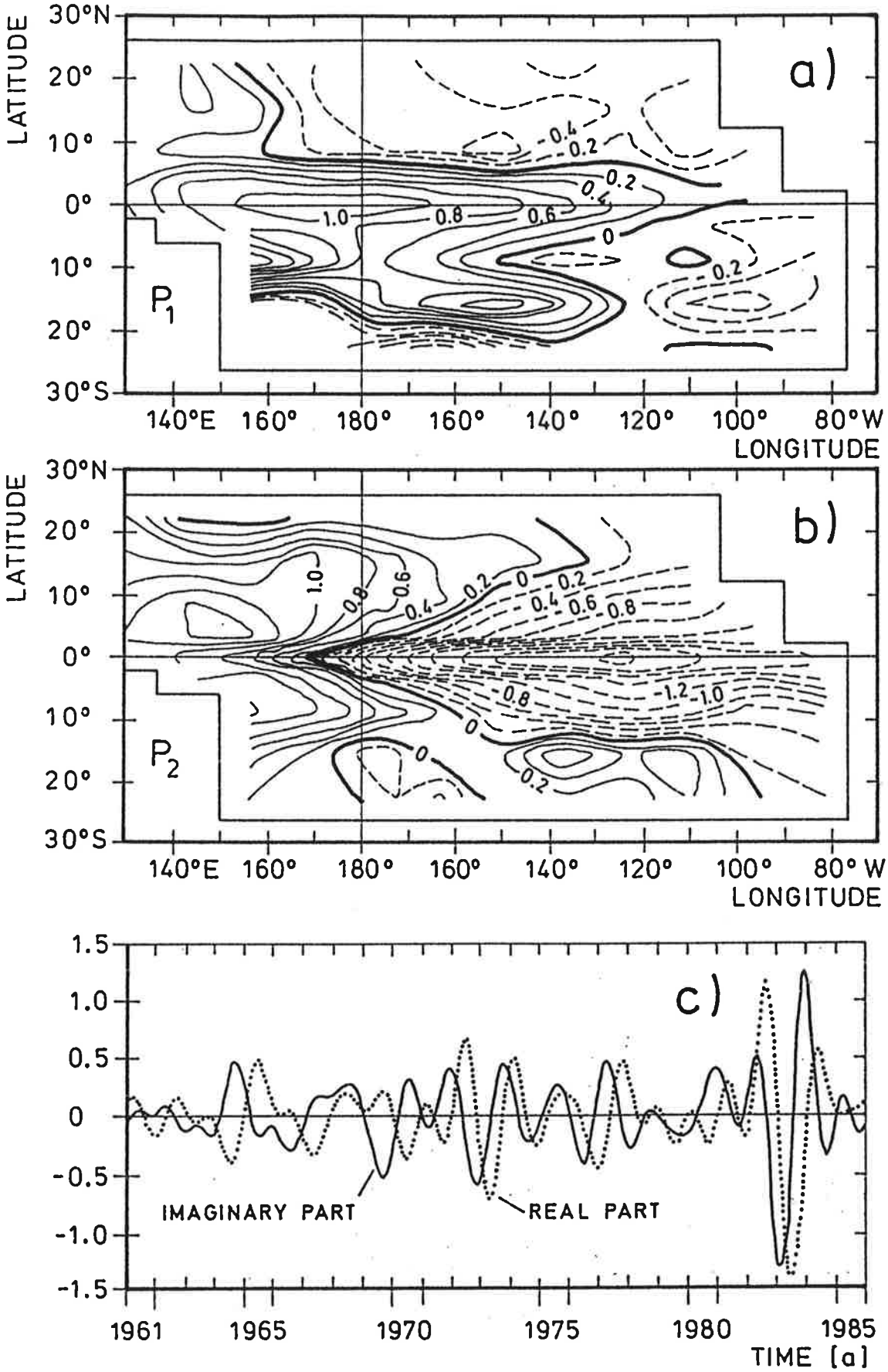

Figure 4: Dominant POP of band pass filtered sea level anomalies simulated in the uncoupled run with observed wind stress. a) Real part, b) Imaginary part, c) Coefficient time series(thick line corresponds to the imaginary part). The time series have been multplied by 17.2.

The overall pattern $\mathbf{p}_2$ is reminiscent of equatorial wave structure and could be interpreted as a Rossby signal located near the western boundary and a Kelvin signal which has already reached the eastern boundary and is being reflected as Rossby and coastal Kelvin waves.

The imaginary part $\mathbf{p}_2$ is followed after a quarter of a rotation period P by the real part $\mathbf{p}_1$. This pattern exhibits positive anomalies along the equator with maximum values near 170°E. These anomalies may be interpreted as a Kelvin wave resulting from Rossby wave reflection of $\mathbf{p}_2$ at the western boundary. A second band of positive anomalies is found south of the equator in the region of the South Pacific Convergence Zone (SPCZ). The negative anomalies of $\mathbf{p}_2$ have moved westward in $\mathbf{p}_1$ at different speeds depending on their latitudinal position: While negative anomalies near 10°N and 10°S are centered in the vicinity of 150°W, those at about 15°N and 15°S are centered at about 100°W. At the northern and southern boundary weak westward propagating boundary Kelvin wave signals can be followed up to about 160°E.

After half a rotation period P, after 13 months, the spatial structure of sea level anomalies is given by $-\mathbf{p}_2$. The positive anomalies at the equator have now propagated farther to the east and have been reflected from the eastern boundary. The positive anomalies in the region of the SPCZ have disappeared (the reasons for this are not clear). Negative anomalies off the equator continue to propagate westward at different speeds, leading to their northeast and southeast orientation. The cycle is completed with pattern $-\mathbf{p}_1$.

In summary, the principal features of the POP mode can be explained by the propagation of equatorial waves and their reflection at meridional boundaries. Although our results support the 'delayed action oscillator' - hypothesis as the ENSO mechanism, we note that the POP accounts for only one third of the low frequency variance, so that there are still important processes missing in explaining ENSO completely.

We will use the findings of this section as a reference with which to compare the results of the coupled experiments.

4. Coupled ocean - atmosphere models

Although the characteristic time scales of ocean and atmosphere are closest at the equator, there is still a well defined gap in their response times. The atmosphere may therefore be described to first order as a steady equilibrium, responding only as a 'slave' to the ocean. We consider two (linear) steady state atmosphere models.

4.1 OGCM - empirical feedback model

In the first model the feedback of the atmosphere on the ocean is described by a linear relation between the stress anomaly field $\underline{\tau}$ at each grid point and the local SST anomaly field T:

$$\underline{\tau} = \underline{\tau}(T) = \underline{a} \cdot T \qquad (3)$$

The set of coefficients $\underline{a}$ was determined empirically by a regression analysis using SST anomalies T from the uncoupled ocean model simulation with observed wind stress (section 3).

To test the regression method we reconstructed stress anomalies $\underline{\tau}$ from the simulated SST anomalies T using (3) and compared them with observed zonal wind stress anomalies at three equatorial locations (Fig. 5). The correspondence of observed and reconstructed zonal wind stress anomalies is in general good, with best agreement in the western and central Pacific (correlation coefficients $r = 0.67$ and 0.51 respectively). The lower correlation in the eastern Pacific ($r = 0.33$) might be attributed partly to the fact that wind stress is almost 'white' in this region (e. g. Wyrtki (1975), Goldenberg and O'Brien (1981)) and is not well correlated with indices of ENSO. In addition the ocean model simulates SST variability in the eastern Pacific less successfully than in the west (Fig. 2).

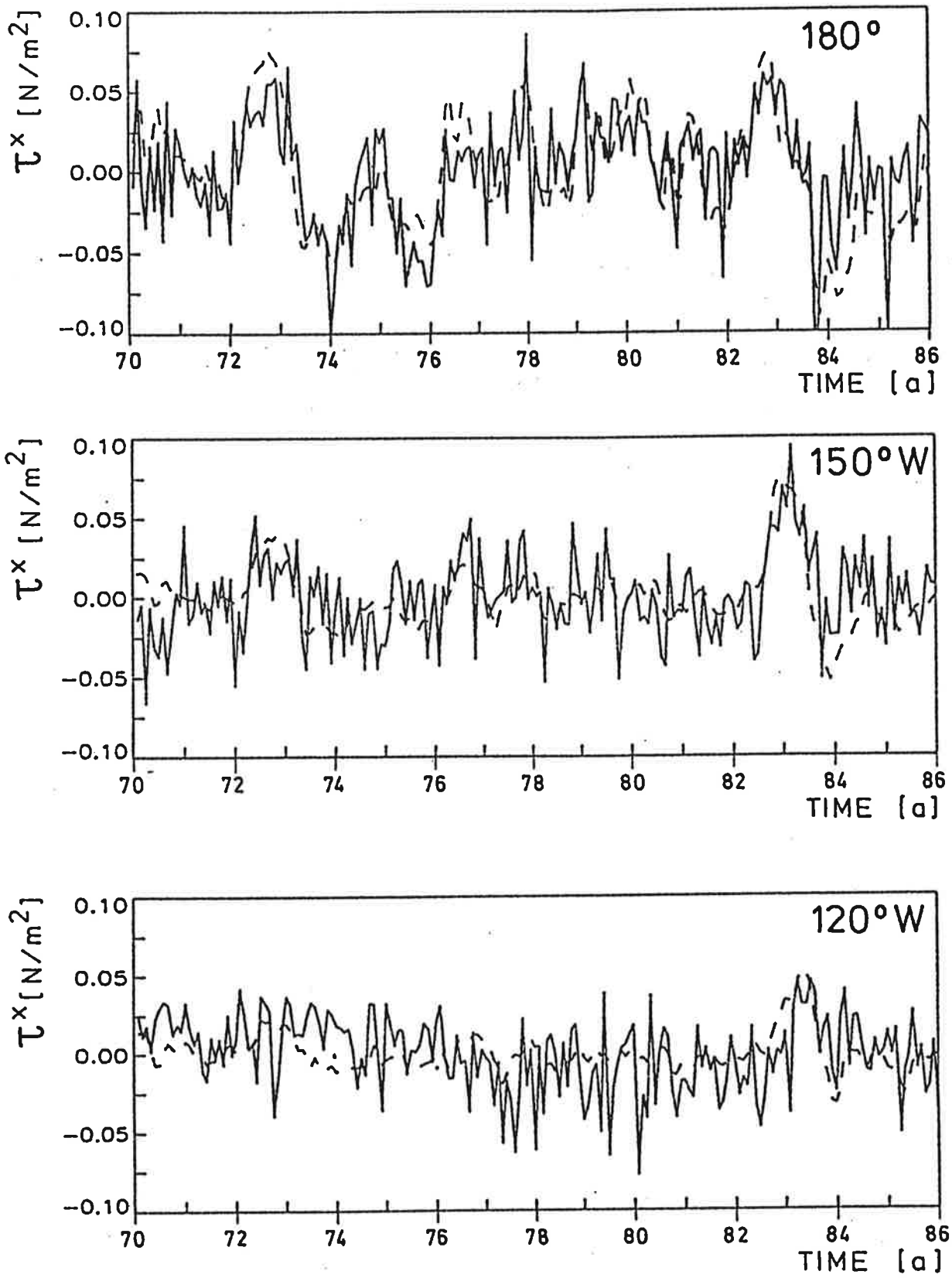

Figure 5: Reconstruction of zonal wind stress anomalies at three equatorial locations using the regression method (3). The reconstructed values have been scaled with 1.5.

To investigate the interannual variability of the coupled model based on (3), we have forced it by purely zonal white noise wind stress forcing with a cosine dependence in the zonal and meridional direction (wavelengths are 240°zonally and 120°meridionally). Maximum anomalies are centered at the dateline at the equator. East of 120°W there is no external forcing.

Initial conditions were taken as those of April 1, 1982 from the uncoupled run with observed wind stress forcing (section 3), corresponding to the situation at the beginning of the 1982/1983 El Niño event.

The coupled system shows considerable low frequency variability during a 16-year integration, which can be inferred from the variance spectrum of sea level anomalies for a location at the equator in the eastern Pacific (Fig. 6). The simulated low frequency variance is approximately doubled compared to that found in a similar uncoupled run without emprirical feedback, which demonstrates the importance of coupled feedbacks for the generation of low frequency variability in the equatorial Pacific.

Fig. 7 shows the dominant POP of sea level anomalies for the 16-year integration. This POP accounts for 50 % of the total (unfiltered) variance and has a rotation time of P = 36 months with a damping time δ = 26 months. It is clearly associated with the low frequency part of sea level variability, as can be inferred from the coefficient time series (Fig. 7c). We can identify three major events, one at the beginning of the integration, one during years 8 and 9, and one at the end of the experiment. The two POP coefficient time series are highly coherent at low frequencies and show a rather constant phase shift of -90° (not shown).

The real and imaginary parts $\mathbf{p}_1$ and $\mathbf{p}_2$ (Figs. 7a and 7b) are very similar to the POP patterns for the uncoupled run with observed wind stress (Fig. 4). Again, pattern $\mathbf{p}_2$ is characteristic for the extreme phases of ENSO, with negative anomalies in the central and eastern equatorial Pacific, surrounded by positve anomalies orientated to the northeast and southeast. Pattern $\mathbf{p}_1$ exhibits positive anomalies along all of the equator and in the region of the SPCZ, and negative anomalies which have propagated westward off the equator. The most important deviations are the splitting of the equatorial maximum near

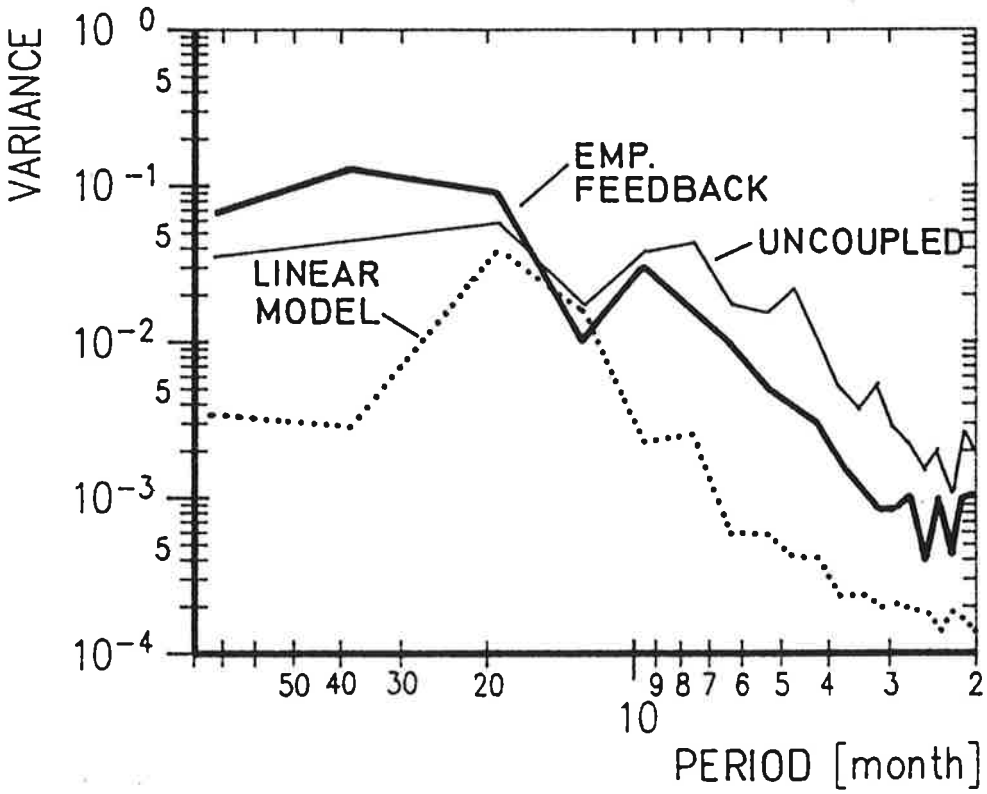

Figure 6: Variance spectra of sea level anomalies at 0°, 110°W for three different experiments. Thick full line: Coupled run with empirical feedback, thin full line: Coupled run with the linear steady state model, dotted line: Uncoupled ocean model forced by white noise. Notice the sharp minimum at the annual period reflecting the removal of the annual cycle.

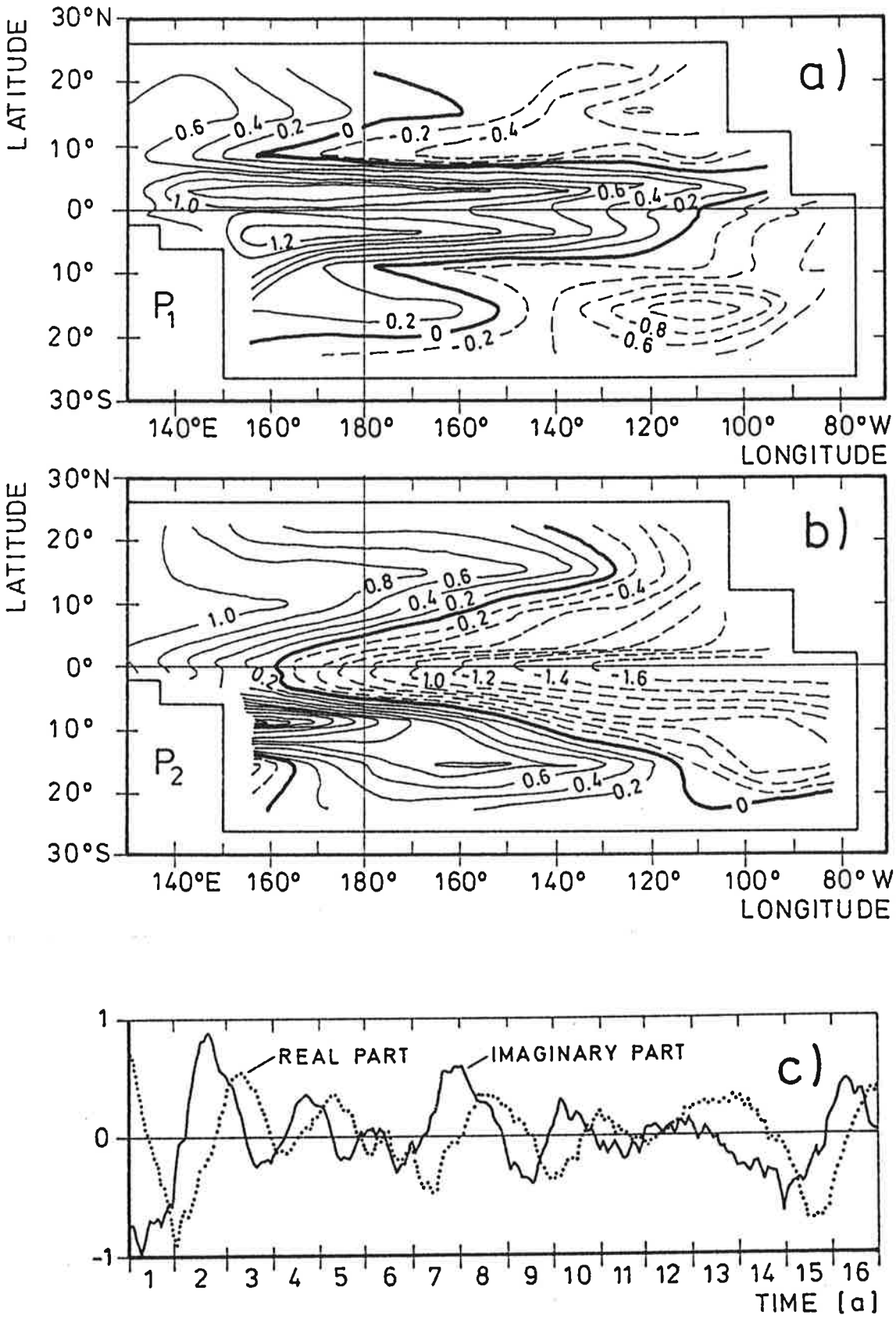

Figure 7: Dominant POP of sea level anomalies in the coupled model using empirical atmsopheric feedback. a) Real part, b) Imaginary part, c) Coefficient time series (thick line corresponds to the imaginary part). The time series have been multiplied by 7.1.

the dateline into two parts and the band of positive anomalies in the region of the SPCZ, which do not extend as far to the southeast as those in the uncoupled reference run.

Considering the extreme simplicity of this coupled model including only linear and local (empirical) atmospheric feedback, its success in simulating low frequency variability in the tropical Pacific is remarkable. The simulated period of 36 months lies within the range of observations, as is the magnitude of typical low frequency changes in sea level with 10 to 20 cm. The coupled model simulation supports the idea that the propagation of equatorial waves is an important contribution to the ENSO mechanism.

4.2 OGCM - linear steady state atmosphere

In the next step we coupled the linear steady state atmosphere model described by Opsteegh and van den Dool (1980) and Opsteegh and Mureau (1984) to our OGCM. This atmosphere model is based on the gouverning physical equations for motions on a rotating sphere. It is linearized around a zonal mean, seasonally varying basic state and has a meridional resolution of 6° and 15 levels in the vertical. Zonally, the variables are represented by Fourier series. We retained waves up to wavenumber $k = 6$.

The ability of the linear steady state atmosphere model to simulate low frequency changes in the near surface wind field was tested by driving it with observed SST anomalies for the period 1970 to 1980 (Reynolds (1988)). The gross features of zonal wind stress variability over the western and central equatorial Pacific are reproduced quite well by the model during the entire 10-year period (Fig. 8). The correlation is largest near the dateline with a value of 0.61. In the vicinity of 120°W, the correlations become rather small. This may be attributed to fluctuations in the location of the zero wind stress line, which cannot be modelled with the low resolution (30°) of the atmosphere model. East of this region correlations are on the order of 0.3. The strength of stress anomalies is simulated reasonably well in the western and central Pacific, but is overestimatd in the east. Outside the equatorial band 5°N -

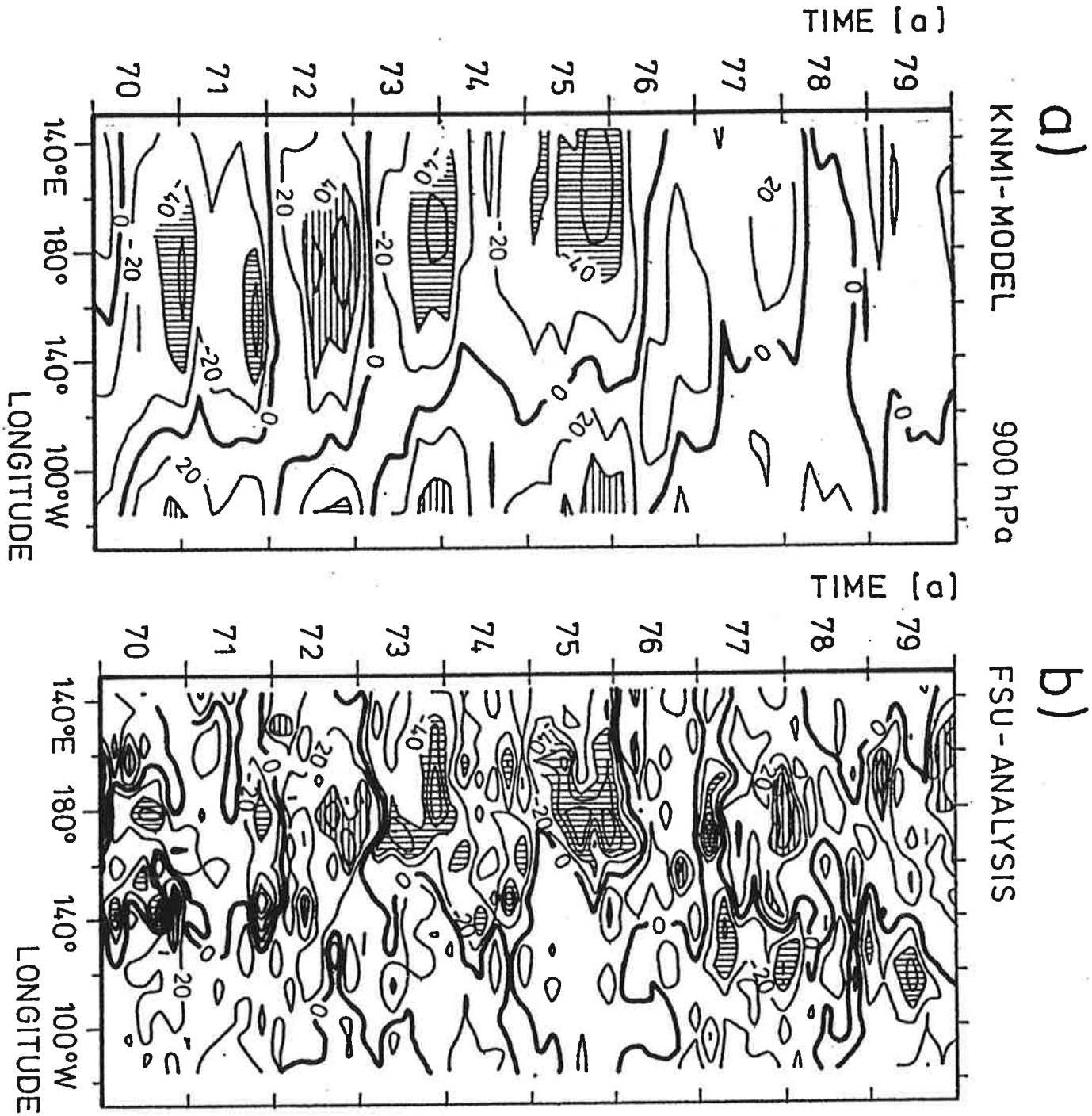

Figure 8: Hovmoeller diagram of zonal stress anomalies (10^3Pa) along the equator. a) Simulated by the linear steady state atmosphere model, b) derived from the FSU analyses.

5°S no significant correlation between simulated and observed zonal wind stress anomalies is found.

The coupling to the ocean model is via the anomalous heating Q and the anomalous surface wind stress $\underline{\tau}$ and linear:

$$Q = a \cdot T \tag{4}$$

$$\underline{\tau} = b \cdot \underline{v} \tag{5}$$

Here the SST anomaly T is defined as the deviation from the mean annual cycle of SST derived from the uncoupled run with observed wind stress (section 3). The anomalous wind stress $\underline{\tau}$ is computed from the anomalous low level wind field $\underline{v}$ at 900 hPa.

The sensitivity of this coupled model to the coupling strength c = (a·b) was investigated in a series of experiments. We found oscillations of various forms depending on c. Below a certain threshold value of the normalized coupling strength K no oscillations occur (K = 1). Here we present one particular run with K = 1.25 in which quasiperiodic oscillations occur (a = $2.25 \cdot 10^{-3}$ kg/(m^2s), b = $7.5 \cdot 10^{-5}$ s^{-1}).

The coupled model was disturbed initially for one month with a strong westerly wind burst over the western Pacific (for details see Latif et al. (1988), who used the same disturbance in a coupled GCM). Thereafter the coupled model was integrated for 16 years without any external forcing.

As in the preceding section POP - analysis was applied to the results. We found one dominant POP with a rotation period P of about 16 months and an e-folding time δ of about 60 months (Fig. 9). The explained variance is 70 %. The POP is very robust. For coupling strengths varying by $\pm$ 20 % the POP analysis gives essentially the same results. The two coefficient time series (Fig. 9c) clearly show a well defined period of 16 months (see also Fig. 6) and a fairly constant phase shift of -90° (as to be expected for the small damping of this oscillation).

The basic spatial features of the POP pair can again be explained by

equatorial ocean wave dynamics. As in the case with empirical feedback, the imaginary part p_2 (Fig. 9b) is similar to the pattern found during the extreme phases of ENSO. The real part p_1, however, shows some significant deviations from the cases of the uncoupled reference run (Fig. 4a) and the empirical feedback (Fig. 7a): There is no uniform sign of anomalies along the equator, the equatorial Kelvin signal in the eastern Pacific extends to the eastern boundary, and the strong signal in the region of the SPCZ is missing.

The most striking difference to the previous two cases, however, is the much shorter oscillation period of only 16 months. A more detailed comparison of the three model simulations gives the impression that Rossby wave activity at higher latitudes is more important in the first two cases, which could explain their longer oscillation period.

There are several possible reasons for the too short oscillation period: The zonal symmetry of the basic state, the neglection of moisture, and the neglection of non-linearities. Further investigation of the model results is therefore needed to explore the nature of the differences in the feedbacks.

Despite the discrepency in oscillation period the experiment presented in this section also supports the 'delayed action oscillator' - hypothesis for ENSO.

5. Summary and discussion

We have investigated the interannual sea level variability simulated with two coupled models and have compared the results with an uncoupled reference run in which the ocean model is forced by observed winds. The main results of this study are:

1. The coupling of ocean and atmosphere is an important contribution for the generation of interannual variability in the equatorial Pacific.

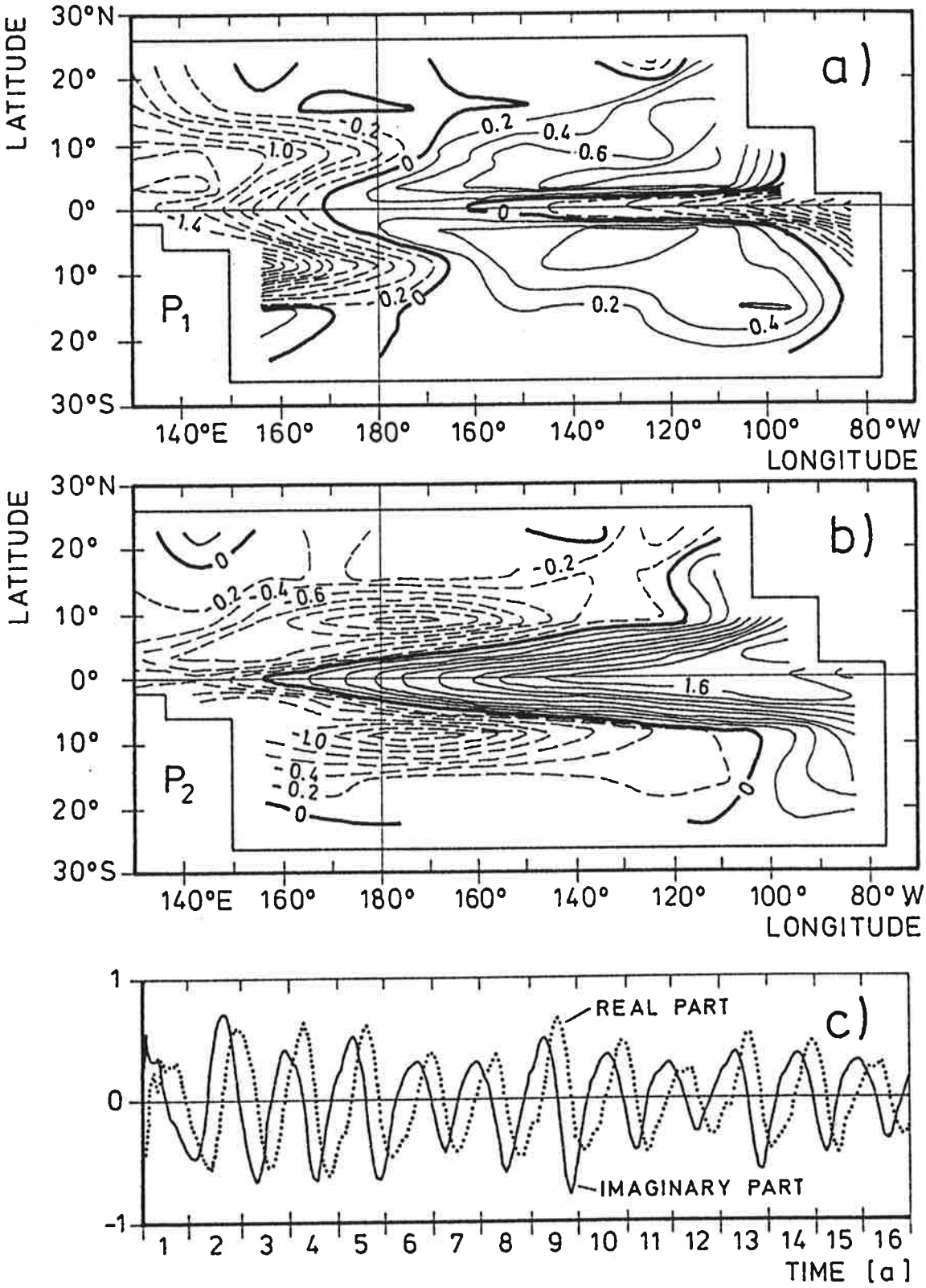

Figure 9: Dominant POP of sea level anomalies in the coupled model using the linear steady state atmosphere model. a) Real part, b) Imaginary part, c) Coefficient time series (thick line corresponds to the imaginary part). The time series have been multiplied by 9.3.

2. A significant contribution to interannual sea level variability (about one third of the total low frequency variance) in the uncoupled reference run can be attributed to a dominant oscillation which can be explained by equatorial ocean wave dynamics.

3. Coupled ocean-atmosphere models including empirical atmospheric feedback can reproduce this wave contribution to interannual variability realistically.

Our model results support the hypothesis that ENSO is strongly gouverned by the propagation of equatorial ocean waves. We note, however, that only one third of the low frequency variance in the uncoupled reference run with observed wind stress forcing is explained by such wave activity. While this part of climate variability in the tropical Pacific can be explained by simplified coupled ocean - atmosphere models only a sophisticated global coupled GCM can be expected to simulate all ENSO mechanisms realistically.

Nevertheless, the success of the coupled model consisting of the OGCM and empirically derived atmospheric feedback in reproducing part of observed interannual sea level variability may be significant for ENSO prediction. We have shown that the spatial structure of sea level anomalies observed during the extremes of ENSO are well reproduced by the second POP pattern of such a coupled model (Figs. 3a and 7b). We may therefore have some confidence that the orthogonal first pattern (Fig. 7a) (with reversed sign) describes the conditions preceding El Niño or La Niña. Since the rotation period P of the dominant POP is about 26 months, these conditions would prevail about half a year before an event has fully developed. These precursers would include anomalies along the equator centered at the dateline and anomalies of the same sign in the region of the SPCZ. Interestingly, van Loon and Shea (1987) have also found evidence for precursers of El Niño located in the region of the SPCZ. The predictive skill of such a coupled system is presently under investigation.

6. Acknowledgements

We wish to thank Prof. Dr. Klaus Hasselmann for suggesting the use of empirical feedback in coupled ocean - atmosphere models. We are indebted to Dr. E. Maier - Reimer for providing the ocean model and for many fruitful discussions. We like to thank also Dr. H. von Storch for many stimulating discussions, Mr. Andreas Schwarz for performing the experiments with empirical feedback and Mrs. Marion Grunert for preparing the diagrams.

REFERENCES

Battisti, D.S. and A.C. Hirst, 1989: Interannual variability in a tropical atmosphere-ocean model: Influence of the basic state, ocean geometry and nonlinearity. J. Atmos. Sci., 46, 1687-1712.

Barnett, T.P., L. Duemenil, U. Schlese, E. Roeckner, M. Latif, 1989: The effect of Eurasian snow cover on regional and global climate variations. J. Atmos. Sci., 6, 661-685.

Goldenberg, S.B., J.J. O'Brien, 1981: Time and space variability of tropical Pacific wind stress. Mon. Wea. Rev., 109, 1190-1207.

Gordon, C., 1988: Coupled model simulation of ENSO (El Niño Southern Oscillation). Phil. Trans. R. Soc. Lond., in press.

Haney, R.L., 1971: Surface thermal boundary condition for ocean circulation model. J. Phys. Oceanogr., 1, 241-248.

Hasselmann, K., 1988: PIPs and POPs: The reduction of complex dynamical systems using principal interaction and oscillation patterns. J. Geophys. Res., 93, 11015-11021.

Hirst, A.C., 1985: Free equatorial instabilities in simple coupled atmosphere-ocean models. Coupled ocean-atmosphere models. J. C. J. Nihoul, Ed., Elsevier Oceanography Ser., 40.

Inoue, M., W.B. White, S.E. Pazan, 1987: Interannual variability in the tropical Pacific prior to the onset of the 1982-83 El Niño. J. Geophys. Res., 92, 11671-116??.

Latif, M., E. Maier-Reimer, D.J. Olbers, 1985: Climate variability studies with a primitive equation model of the equatorial Pacific. Coupled ocean-atmosphere mosdels. J. C. J. Nihoul, Ed., Elsevier Oceanography Ser., 40.

Latif, M., 1987: Tropical ocean circulation experiments. J. Phys. Oceanogr. 17, 246-263.

Latif, M., J. Biercamp, H. v. Storch, 1988a: The response of a coupled ocean-atmosphere general circulation model to wind bursts. J. Atmos. Sci., 45, 964-979.

Lau, K.M., 1985: Elements of a stochastic dynamical theory of the long-term variability of the El Niño/Southern Oscillation. J. Atmos. Sci., 42, 1552-1558.

Legler, D.M., J.J. O'Brien, 1984: Atlas of tropical Pacific wind stress climatology 1971-1980. - Florida State University, Department of Meteorology, Tallahassee FL 32306, 182 pp.

Neelin, J.D., 1988: Interannual oscillations in an ocean GCM-simple atmosphere model. Phil. Trans. R. Soc. Lond., in press.

Opsteegh, J.D. and H.M. van den Dool, 1980: Seasonal differences in the stationary response of a linearized primitive equation model: Prospects for long-range weather forecasting? J. Atmos. Sci., 37, 2169-2185.

Opsteegh, J.D. and R. Mureau, 1984: Description of a 15-layer steady state atmosphere model. University of Maryland, Department of Meteorology, College Park, MD 20742, U. S. A..

Pacanowski, R.C. and S.G.H. Philander, 1981: Parameterization of vertical mixing in numerical models of tropical oceans. J. Phys. Oceanogr., 11, 1443-1451.

Philander, S.G.H., N.C. Lau, R.C. Pacanowski, M.J. Nath, 1988: Two different simulations of the Southern Oscillation and El Niño with coupled ocean-atmosphere general circulation models. Phil. Trans. R. Soc. Lond., in press.

Schopf, P.S. and M.J. Suarez, 1988: Vacillations in a coupled ocean-atmosphere model. J. Atmos. Sci., 45, 549-566.

Storch, H.v., T. Bruns, I. Fischer-Bruns, K. Hasselmann, 1988: Principal Oscillation Pattern analyses of the 30-60 day oscillation in a GCM equatorial troposphere. J. Geophys. Res., 93, 11022-11036.

Van Loon, H. and D.J. Shea, 1987: The Southern Oscillation. Part VI: Anomalies of sea level pressure on the Southern Hemisphere and of Pacific sea surface temperature during the development of a warm event. Mon. Wea. Rev., 115, 370-379.

White, W.B. and S.E. Pazan, 1987: Hindcast/Forecast of ENSO events based upon the redistribution of observed and model heat content in the western tropical Pacific, 1964-86. J. Phys. Oceanogr., 17, 264-280.

Wyrtki, K., 1985: Water displacements in the Pacific and the genesis of El Niño cycles. J. Geophys. Res., 90, 7129-7132.

Xu, J.S. and H.v. Storch, 1989: "Principal Oscillation Pattern" - Prediction of the state of ENSO. J. Climate, submitted.

Zebiak, S.E. and M.A. Cane, 1987: A model El Niño-Southern Oscillation. Mon. Wea. Rev., 115, 2262-2278.